



Wireless Closed-Loop Optical Regulation System for Seizure Detection and Suppression *In Vivo*

Yamin Li^{1,2†}, Shengwei Xu^{2,3†}, Yang Wang^{1,2}, Yiming Duan^{2,3}, Qianli Jia^{2,3}, Jingyu Xie^{2,3}, Xiaowei Yang¹, Yiding Wang^{2,3}, Yuchuan Dai^{2,3}, Gucheng Yang^{2,3}, Miao Yuan^{1,2}, Xiaoting Wu^{1,2}, Yilin Song^{2,3}, Mixia Wang^{2,3}, Hongda Chen^{1,2}, Yijun Wang^{1,2}, Xinxia Cai^{2,3*} and Weihua Pei^{1,2,4*}

¹State Key Laboratory on Integrated Optoelectronics, Institute of Semiconductors, Chinese Academy of Sciences, Beijing, China, ²Institute of Semiconductors, University of Chinese Academy of Sciences, Beijing, China, ³State Key Laboratory of Transducer Technology, Aerospace Information Research Institute, Chinese Academy of Sciences, Beijing, China, ⁴CAS Center for Excellence in Brain Science and Intelligence Technology, Shanghai, China

OPEN ACCESS

Edited by:

Deqiang Wang,
Chongqing Institute of Green and
Intelligent Technology (CAS), China

Reviewed by:

Yuxiao Yang,
University of Central Florida,
United States
Mohammad Ismail Zibaii,
Shahid Beheshti University, Iran

*Correspondence:

Xinxia Cai
xxcai@mail.ie.ac.cn
Weihua Pei
peiwh@semi.ac.cn

[†]These authors have contributed
equally to this work

Specialty section:

This article was submitted to
Biomedical Nanotechnology,
a section of the journal
Frontiers in Nanotechnology

Received: 06 December 2021

Accepted: 07 February 2022

Published: 11 March 2022

Citation:

Li Y, Xu S, Wang Y, Duan Y, Jia Q, Xie J,
Yang X, Wang Y, Dai Y, Yang G,
Yuan M, Wu X, Song Y, Wang M,
Chen H, Wang Y, Cai X and Pei W
(2022) Wireless Closed-Loop Optical
Regulation System for Seizure
Detection and Suppression *In Vivo*.
Front. Nanotechnol. 4:829751.
doi: 10.3389/fnano.2022.829751

There are approximately 50 million people with epilepsy worldwide, even about 25% of whom cannot be effectively controlled by drugs or surgical treatment. A wireless closed-loop system for epilepsy detection and suppression is proposed in this study. The system is composed of an implantable optrode, wireless recording, wireless energy supply, and a control module. The system can monitor brain electrical activity in real time. When seizures are recognized, the optrode will be turned on. The preset photosensitive caged compounds are activated to inhibit the seizure. When seizures are inhibited or end, the optrode is turned off. The method demonstrates a practical wireless closed-loop epilepsy therapy system.

Keywords: seizure, optrode, wireless, local field potential (LFP), caged compounds

1 INTRODUCTION

Epilepsy is a chronic brain disease characterized by transient central nervous system dysfunction caused by the abnormal discharge of brain neurons. Clinical manifestations are symptoms of motor, sensory, consciousness, and neural dysfunction (Mormann et al., 2006; Sterbova et al., 2018). It affects approximately 50 million people worldwide, of which 25% have intractable epilepsy (Bordey, 2021; Gao et al., 2021). For patients with intractable epilepsy, even the maximum dose of drugs cannot fully inhibit seizures. The absorption and accumulation of antiepileptic drugs will lead to significant side effects (Hoffman et al., 2020). Surgery is an effective therapy in the treatment of refractory epilepsy. However, it has certain risks and easily produces sequelae (Dai et al., 2020).

In recent years, researchers have devoted themselves to exploring other treatments for epilepsy. Hristova et al. (2021) demonstrated that the optogenetic method could shorten seizures. The optogenetic method can only be tested in animal models, the application of which in humans is limited. Vagus nerve stimulation, transcranial magnetic stimulation, deep brain stimulation, external electric field stimulation, and deep anesthetic treatment are also widely used in the treatment of epilepsy (Rossetti et al., 2004; Kawai, 2008; Krishna and Lozano, 2014; Klinger and Mittal, 2018; Yang et al., 2019; Hu et al., 2020; Tsai et al., 2020). The parameters of these electric stimulation therapies need to be continuously adjusted according to the patients and treatment stages (Sun and Morrell, 2014; Zheng et al., 2019; Takeuchi et al., 2021).

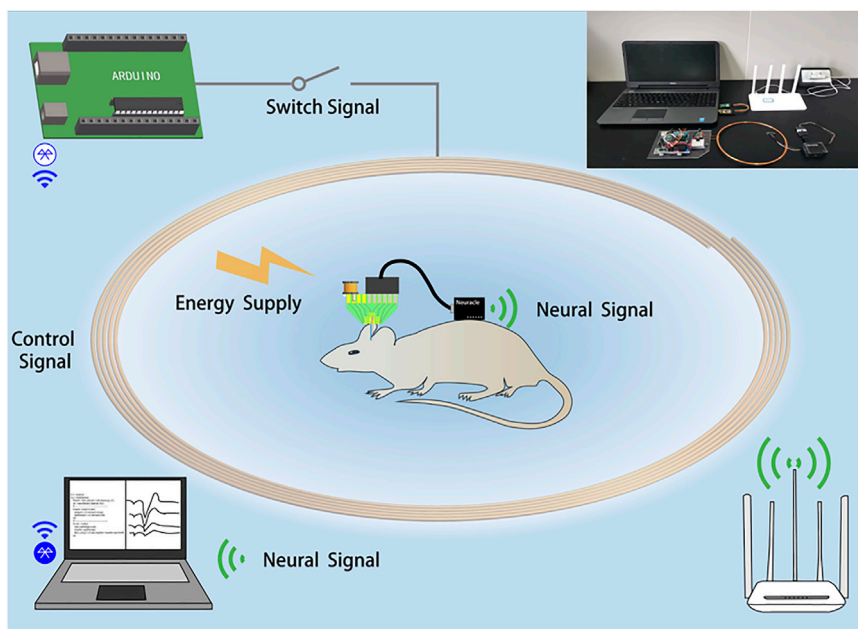


FIGURE 1 | System block diagram of the wireless closed-loop system for epilepsy detection and suppression. The illustration is a physical picture.

Caged compounds, including caged- γ -aminobutyric acid (GABA), such as ruthenium-bipyridine-triphenylphosphine-c-GABA (RuBi-GABA), can be activated with light in epilepsy treatment (Trigo et al., 2009; Lopes-dos-Santos et al., 2011). Caged compounds are generally neurotransmitters or natural proteins that can be absorbed by neurons quickly. Yang et al. (2012) reported that RuBi-GABA with blue light could quickly terminate the seizure activity. In the years that followed, the team optimized the optimal concentration and light intensity of RuBi-GABA to achieve the best inhibition effect (Wang et al., 2017). RuBi-GABA contains a photolabile protecting group that can be removed by exposure to light. Combined with RuBi-GABA and light, targeted treatment of epilepsy inhibition can be realized (Rothman et al., 2007; Yang et al., 2010). However, seizures are identified by people and then give light to release RuBi-GABA manually at present.

In this study, a closed-loop optical regulation system of seizure detection and wireless light-controlled RuBi-GABA inhibition is proposed. The effect of real-time seizure detection and suppression is demonstrated *in vivo*. The system dramatically shortens the seizure time. The wireless and closed-loop optical regulation system provides a new method for epilepsy treatment.

2 MATERIALS AND METHODS

2.1 Reagents and Apparatus

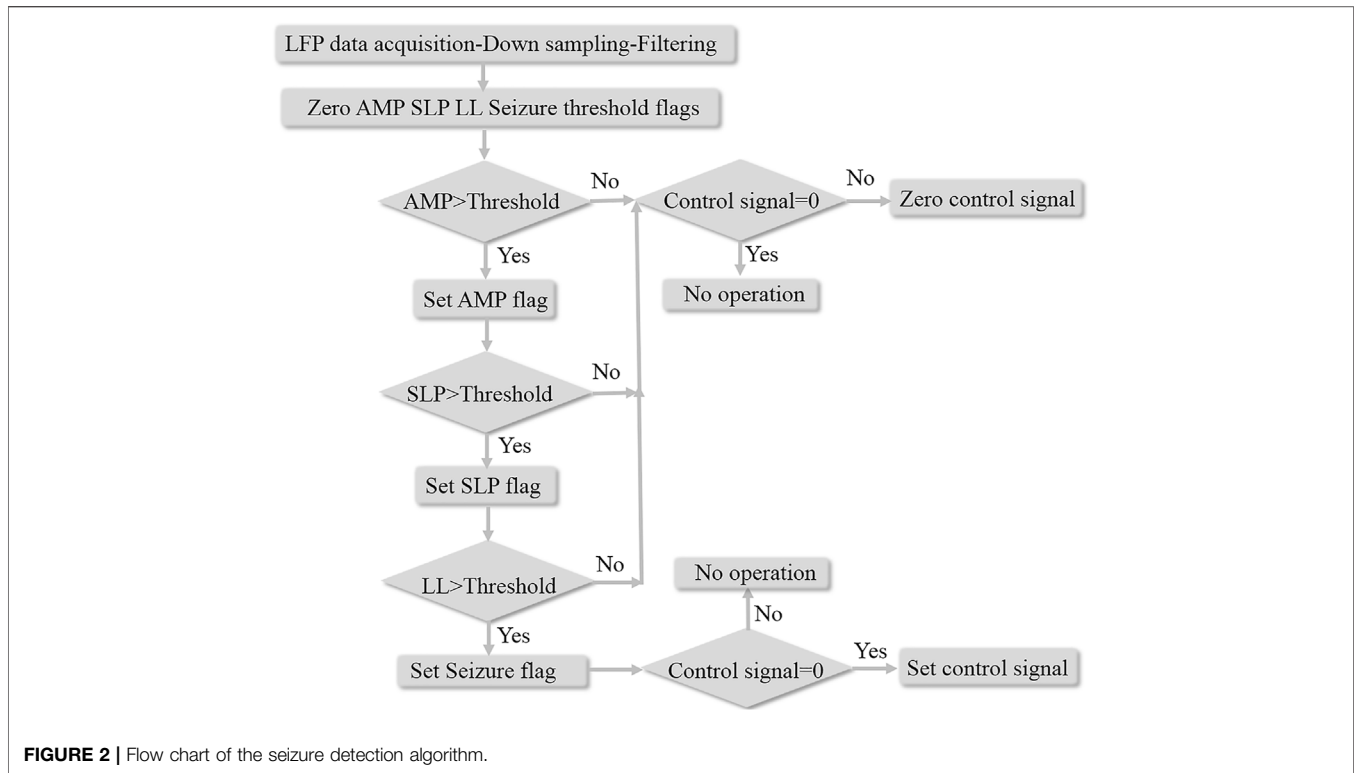
Anhydrous lithium chloride (LiCl), pilocarpine hydrochloride, and scopolamine methyl bromide were purchased from Macklin Biochemical Corporation (China). RuBi-GABA was obtained from Tocris Bioscience (Missouri, United States). Saline (0.9% NaCl), red glue (LOCTITE 3611), and AB glue (Kafuter) were

obtained from Shuang He Corporation (China). Phosphate-buffered saline (PBS, 0.1 M, pH 7.4) was obtained from Sigma (China).

The instruments used in the experiment were an electrochemical workstation (HUACHEN CHI660D, China), a source meter (KEITHLEY 2450, United States), infrared thermal imager (Fotric 220 s United States), optical power meter (THORLABSPD100D probe S142C, United States), and chemical vapor deposition apparatus (Specialty Coating Systems PDS 2010, United States). Animals in the study were anesthetized by using an isoflurane anesthesia machine (RWD520, RWD Life Science, China).

2.2 Wireless Closed-Loop Optical Regulation System

The wireless closed-loop optical regulation system for seizure detection and suppression (WLCS) can be divided into two parts: an implanted part and an external part. The implanted part is a homemade optrode consisting of a microelectrode array (MEA) and an LED probe. The external part is composed of the wireless recording, wireless energy supply, and control module, as shown in **Figure 1**. The optrode records the local field potential (LFP) and gives light to the specified area. The wireless recording module (Neuracle, China) is used to amplify the LFP and transmit it to the control module. The control module is used to receive, analyze the LFP, and send signals to turn on or off the optrode. The control module is composed of a circuit and a laptop. The circuit is composed of a single-chip microcomputer (Arduino UNO R3, Italy) and one relay (Juying electronic, China), which is used to receive the signal sent by the computer and control the opening and closing of the wireless



energy supply system. The wireless energy supply module (XKT801-05, China) provides energy for the optrode through the principle of electromagnetic induction to generate the LED light. The wireless energy supply system consists of two parts: the transmitter circuit uses a chip to generate an alternating current (AC) signal of 180 kHz. Then, this signal is amplified by an amplifying circuit to supply power to the inductor. The inductance is 13 μH with 20 cm in diameter and wound by a copper wire with a diameter of 1 mm. The receiver circuit uses the LC (C:330 pF in 0402 L; 2.2 mH in CD43) network to receive energy from the optrode.

The LFP during seizures has the characteristics of high frequency and large amplitude. Three characteristic parameters, amplitude (AMP), slope (SLP), and line length (LL) are defined to make predictions. When the LL is greater than a threshold, it can be preliminarily determined as a seizure. LL alone as a criterion may lead to misjudgments. To enhance the algorithm's robustness, the amplitude (AMP) and slope (SLP) of the LFP are added as criteria. The calculation formulas of AMP, SLP, and LL are as follows (White et al., 2006; Xu et al., 2019):

$$\text{AMP} = \frac{1}{N} \sum_{i=1}^N \text{abs}[x(i)], \quad (1)$$

$$\text{SLP} = \frac{\text{Max}[x(i)] - \text{Min}[x(j)]}{|i - j|}, \quad (2)$$

$$\text{LL} = \sum_{i=1}^{N-1} \text{abs}[x(i+1) - x(i)], \quad (3)$$

where N represents the length of the data window, and $x(i)$ represents the sampling data.

The key to accurately judging seizures lies in the determination of three thresholds. In the experiment, the LFP in the normal state was recorded for at least 10 min, and three characteristic parameters were calculated every 5 s. The average values (A_{AMP} , A_{SLP} , and A_{LL}) and standard deviation (S_{AMP} and S_{SLP}) of AMP, SLP, and LL are obtained. The thresholds for seizures are set as follows, where d is an integer and k is also an integer:

AMP threshold:

$$T_{AMP} = A_{AMP} + S_{AMP} \times d. \quad (4)$$

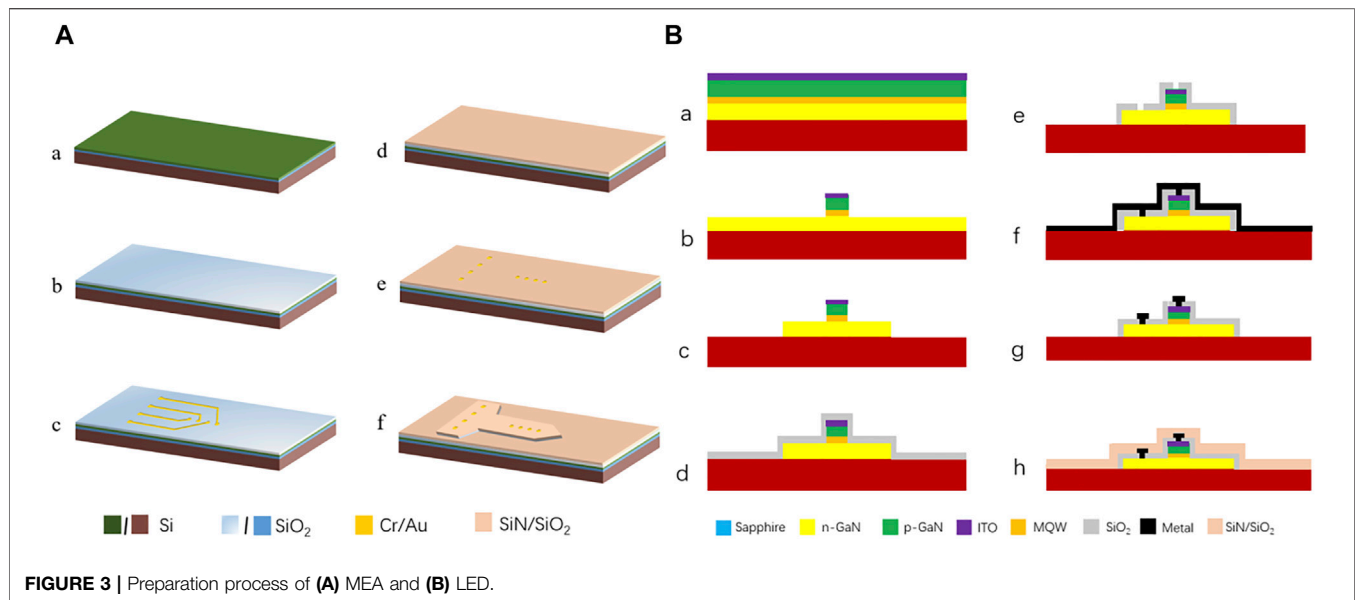
SLP threshold:

$$T_{SLP} = A_{SLP} + S_{SLP} \times d. \quad (5)$$

LL threshold:

$$T_{LL} = A_{LL} \times k. \quad (6)$$

The LFP is collected through the wireless EEG recording system. The sampling frequency is 1 kHz, and the flow chart of the seizure detection algorithm is shown in **Figure 2**. The collected signals are processed by down acquisition (250 Hz), filtering (2–100 Hz), and notching (50 Hz). The AMP, SLP, and LL of the LFP are calculated every 5 s and compared with the thresholds; when the AMP, SLP, and LL are greater than the corresponding threshold simultaneously, set the seizure flag and the wireless energy supply signal to 1. Then, the relay is turned on to make the wireless energy supply system work. The optrode is light on, and RuBi-GABA is active.



2.3 Design, Fabrication, and Assembly of the Optrode

2.3.1 Microelectrode Array Fabrication Process

The optrode is fabricated by integrating a silicon microelectrode array (MEA) with an LED probe. The size of the recording point on silicon MEA is 20 μm , the spacing between recording points is 200 μm , and the length is 5 mm. The detailed preparation process is shown in our previous study (Chen et al., 2014). The straightforward fabrication process is demonstrated in **Figure 3A**: the SOI wafer is cleaned with standard methods; SiO_2 is oxidized as the lower insulating layer; the metal is deposited and is patterned by stripping; the $\text{SiO}_2/\text{SiN}_x/\text{SiO}_2$ insulating layer is grown as the upper insulating layer; recording points and solder joints are exposed; photoresist is used as a mask layer, and the needle shape is etched; and the MEA is released from the silicon wafer.

2.3.2 LED Fabrication Process

The LED probe was prepared on a sapphire substrate with a needle length of 5.5 mm, a width of 195 μm , and a luminous surface size of 87.5 $\mu\text{m} \times 4000 \mu\text{m}$. The preparation process is shown in **Figure 3B**. For the specific preparation process, please refer to the study published by our group (Zhang et al., 2016; Li et al., 2021), briefly introduced as follows: a. indium tin oxide (ITO) is grown on the cleaned sapphire epitaxial wafer; b. the P-type luminous area is defined; c. N-type mesa is defined; d. SiO_2 is deposited as the passivation layer; e. photolithography passivation layer to corrode SiO_2 ; f. metal lines are patterned, and metal electrodes are allowed to evaporate; g. the metal is peeled off of the nonelectrode; h. the insulating layer is evaporated by PECVD; finally, the LED is released by laser cutting. Then, parylene was grown as an anti-liquid penetration layer.

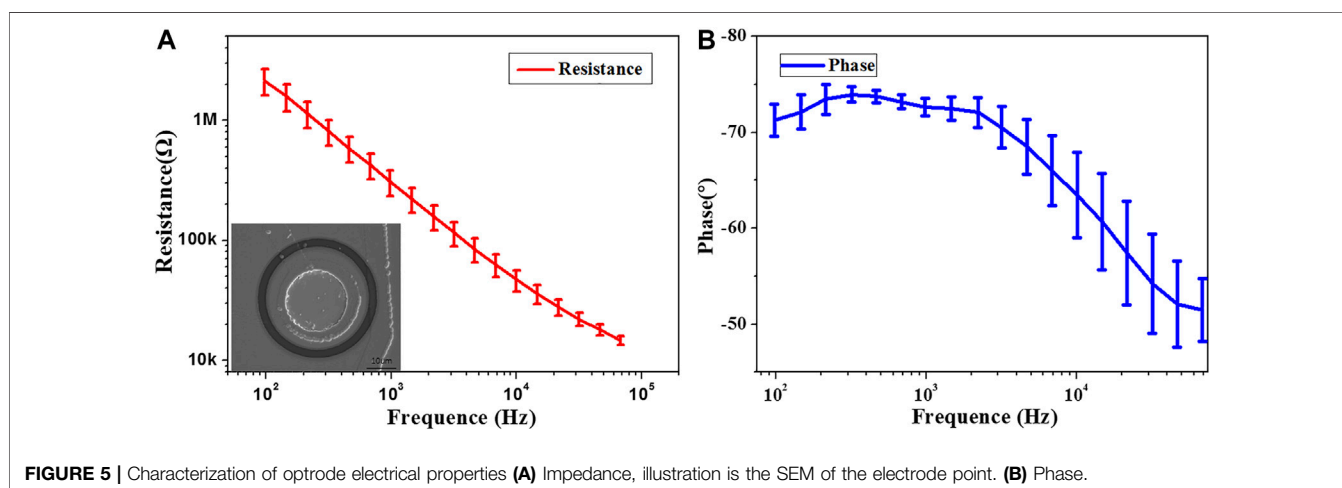
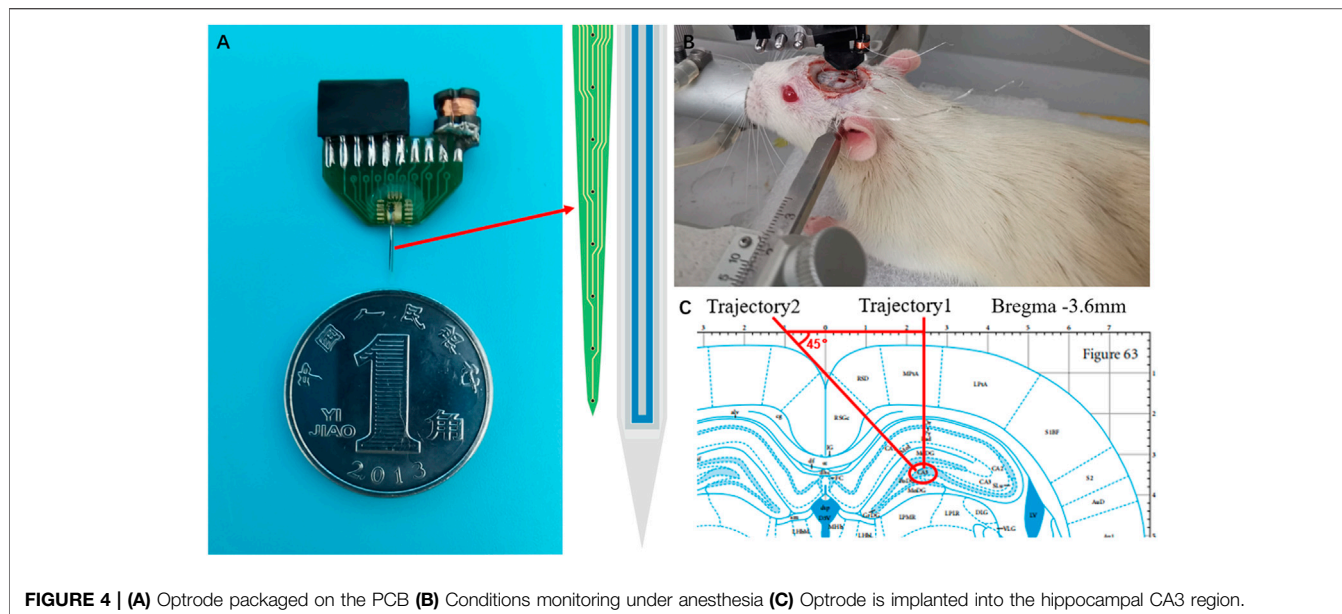
2.3.3 Integration of MEA and LED Probes

MEA and LED probes are pasted on a printed circuit board (PCB) with red glue under an operating microscope. The MEA and LED probes need to be closely adjacent to reduce implantation damage. The MEA and LED probes are connected to the PCB through gold wires and used for signal transmission and LED power supply. At the same time, the power receiving module (inductance and capacitance) is welded on the PCB. Finally, waterproof resin is used to seal the circuit. **Figure 4A** shows the optrode packaged on the PCB, and the sealed device is shown in **Figure 4B**.

2.4 In Vivo Experiments

Male Sprague–Dawley rats (250–300 g, 8–10 weeks) were purchased from Vital River Laboratory Animal Technology Co., Ltd. (Beijing, China) for epilepsy modeling. All rats were placed in a 12-hour light/dark cycle with temperature and humidity maintained at $22 \pm 2^\circ\text{C}$ and $40 \pm 5\%$. All experiments were performed with the permission of the Beijing Association on Laboratory Animal Care, license number SYXK(JING)2020-0045.

Temporal lobe epilepsy (TLE) is a recurrent and unpredictable neurological disorder which is associated with dysfunction of neuronal circuits in the hippocampus (Janz et al., 2017). In this study, we built the TLE model as follows: Lithium chloride (127 mg/kg) was injected intraperitoneally into rats. After a duration of 18–20 h, scopolamine (1 mg/kg, i. p.) was injected to reduce cholinergic injury of the peripheral blood to the nervous system, and pilocarpine (10 mg/kg, i. p.) was injected 30 min later. Rats with stage IV or V seizures within 30 min after pilocarpine injection were considered as successful TLE epilepsy models. They were tested when they entered the incubation period.

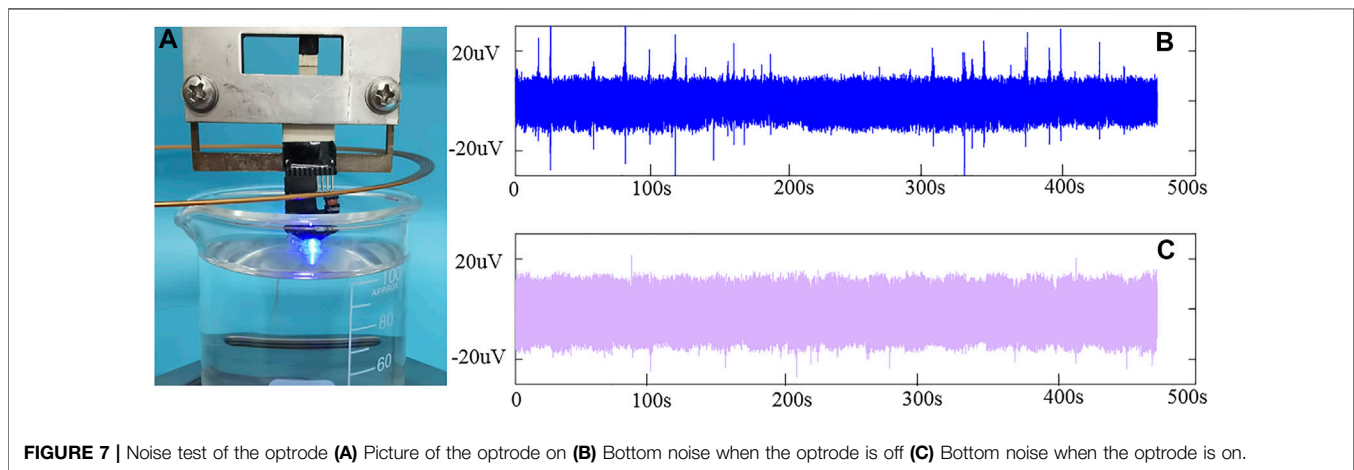
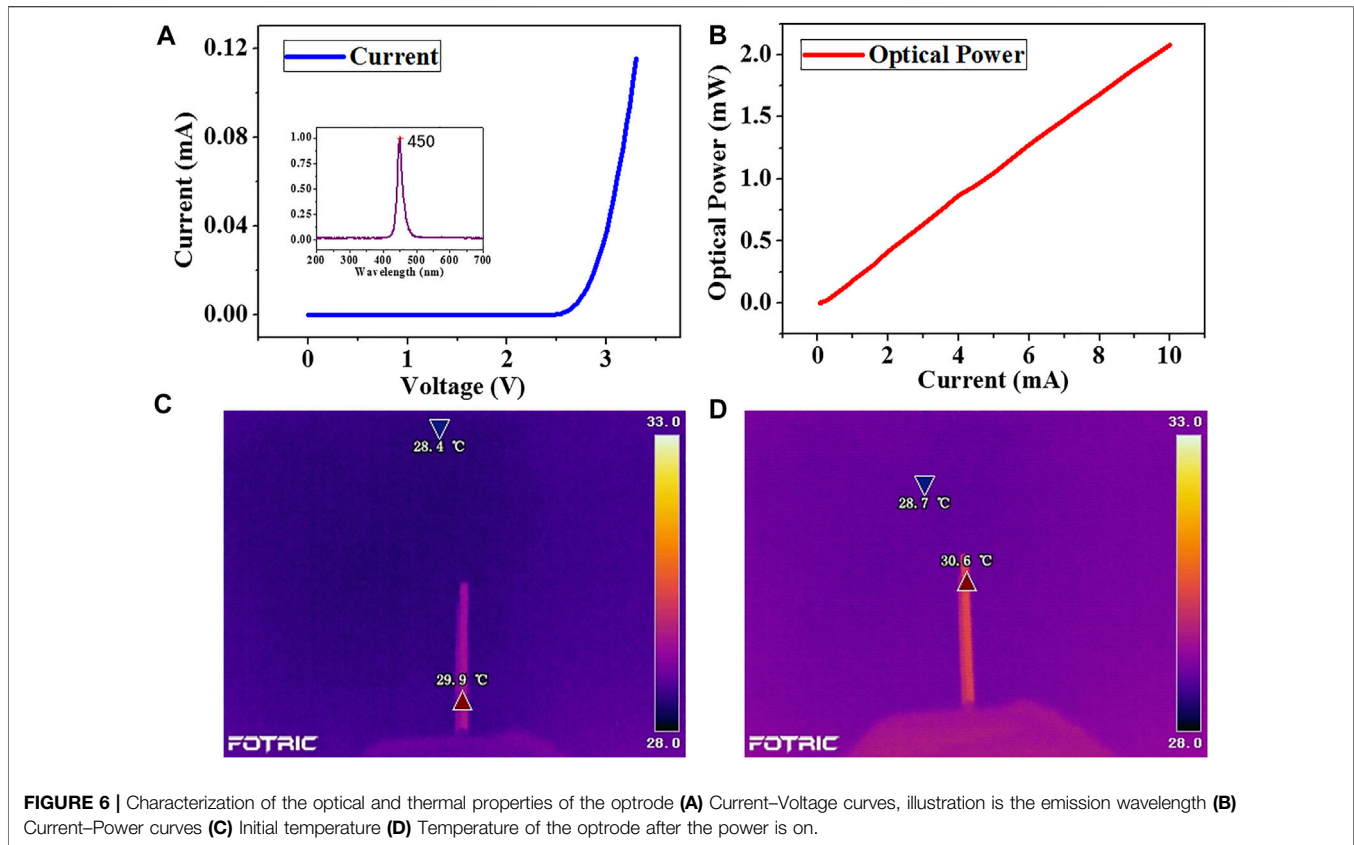


The rats were fixed on a stereotactic platform. Craniotomy was performed under isoflurane anesthesia. Isoflurane at a 4–5% concentration was used for induction, and 0.5–2% was used to maintain general anesthesia. Meanwhile, the rats were warmed with a 37°C heating pad. A stainless steel nail is fixed to the skull above the cerebellum to connect the ground wire and reference line. According to the rat brain atlas of Pacinos and Watson, one position of the drilling hole is AP–3.6 mm, ML 2.2 mm, which is used to implant the optrode into the CA3 of the hippocampus, according to trajectory 1, and the other position is AP–3.6 mm, ML–1.0 mm, which is used to inject the RuBi-GABA solution, according to trajectory 2, as shown in **Figures 4B,C**. 20 μ L of the RuBi-GABA solution (5 mM, dissolved in normal saline) was microinjected *via* a syringe pump in the dim circumstance with a red lamp. In addition, 20 μ L of normal saline was injected instead in the control experiment.

3 RESULTS

3.1 Characterization of the Optrode Performance

The impedance of the optrode determines the signal-to-noise ratio of the recorded LFP. The platinum electrode and the optrode were inserted into 0.1 M phosphoric acid buffer to test the impedance at frequencies from 1 Hz to 100 kHz. The three-electrode test system was used to measure the impedance of the optrode, in which the platinum electrode is used as the reference electrode and the counter electrode. The results are shown in **Figure 5**. The impedance and phase meet the requirements of neural signal recording (Kozai et al., 2016; Schander et al., 2016). The micro morphology of the electrode is shown in **Figure 5A** through a SEM (scanning electron microscope).



The optical and thermal performances of the optrode are characterized. It can be seen from **Figure 6** that the turn-on voltage of the optrode is approximately 2.6 V. The optical power increases linearly with the increasing current, providing enough optical power required for RuBi-GABA activation. The optrode cannot convert all the electrical energy into light energy. It will cause the temperature to rise in the brain, which directly or indirectly affects the action potential and the LFP of neuronal groups (Long and Fee, 2008). It is generally considered that a temperature rise $<1^{\circ}\text{C}$ is acceptable (Shen and Schwartzkroin,

1988). The temperature is 29.9°C with the optrode off and rises to 30.6°C when the optrode is derived with a voltage of 2.8 V. The heat dissipation in the brain is better than that in the air. Therefore, it is considered that the optrode's temperature rise is negligible.

The amplitude of the LFP is commonly approximately $10\text{--}1000\ \mu\text{V}$, and it is easily disturbed by noise (Santhanam et al., 2006). When recorded with the optrode, the external power supply and the light will interfere with the recording of the LFP. To assess the interference, the optrode is inserted into

TABLE 1 | Effect of the threshold on seizure detection.

Parameter value	False detection rate (1 channel)	False detection rate (≥ 4 channel)	Detection rate (1 channel)	Detection rate (≥ 4 channel)
$d = 1, k = 1$	0.37	0.42	0.78	0.86
$d = 2, k = 1$	0.23	0.214286	0.78	0.85
$d = 3, k = 1$	0.20089286	0.142857	0.77	0.84
$d = 3, k = 2$	0	0	0.74	0.80
$d = 3, k = 3$	0	0	0.73	0.79

the PBS solution to simulate the internal environment. The noise floor is recorded when the optrode is turned on and off. Then, the data pass through a bandpass filter (1–200 Hz). The filtered data are shown in **Figure 7**. The noise floor is approximately $10 \mu\text{V}$ when the optrode is off. When the wireless energy supply system works and the optrode lights up, the noise floor is probably $15 \mu\text{V}$. By comparison, noise will be introduced when the wireless energy supply system is working and the optrode is turned on. However, the influence is relatively small, and a good signal-to-noise ratio can still be obtained.

3.2 Analysis of the Threshold Value

Threshold affects the accuracy of seizure detection. It can be seen from the threshold formula that the values of parameters d and k affect the threshold. Seizures are determined only when the *AMP*, *SLP*, and *LL* exceed the threshold entirely. While paying attention to the seizure detection rate, we also showed solicitude for the false detection rate of the seizure (determining the normal signal as the epileptic signal). The values of d and k affect the true detection rate and false detection rate of seizures. The greater the values of d and k , the greater are the thresholds of *AMP*, *SLP*, and *LL*. Eight channels of LFP data were collected in the experiment. Because each channel is located in different positions of the rat brain, we calculated the threshold of each channel separately. **Table 1** shows the effect of the threshold on seizure detection of one channel and more than four channels. **Table 1** shows that with increasing d and k , the detection rate and false detection rate of seizures decrease at the same time. For the same parameter, the detection rate of more than four channels is higher than that of one channel, and the false detection rate is lower. Seizures are determined only when more than half of the channels detect seizures, further ensuring a high detection rate and low false detection rate. When epilepsy occurs, the optrode will be turned on, and the drug will be released. To reduce drug release mistakenly, we adopted threshold parameters ($d = 3$ and $k = 2$) in real-time detection.

3.3 Analysis of Normal and Seizure Activities in the Acute TLE Model

The LFP can be used to judge whether epilepsy occurs. The experiment results for the control group just for optical stimulation with saline injected are shown in **Supplementary Figure S1**. **Supplementary Figure S1** shows the local field potential (LFP) of a channel. When no RuBi-GABA was injected and only saline was injected, it will not affect the epileptic activity. In the experiment, the LFP of rats in the normal, seizure, and RuBi-

GABA release was recorded, as shown in **Figure 8**. During seizures, rats have apparent convulsions and salivation, sometimes accompanied by a squeak. To verify whether RuBi-GABA works after light irradiation, we used a self-control approach. First, the relay is de-energized manually, and seizures are allowed to last for a while. Combined with animal behavior and seizure detection algorithms, the time of seizure occurrence can be determined. As shown in **Figure 8**, compared with the normal signal, the signal amplitude and frequency increased significantly during seizures. Before light was given, seizures continued. After the seizure lasted a few minutes, the relay is energized manually. Then, the algorithm detected the seizure, the wireless energy supply system started to provide energy, and the receiving coil received energy to light the optrode. The intensity is 1.03mW . After 10 s of illumination, the amplitude and frequency of the LFP decreased, which is due to the release of RuBi-GABA which can be activated with light in epilepsy treatment, and the algorithm detected that seizures stopped. The control signal was sent to the off state, and the wireless energy supply system stopped working. It can also be seen from the behavior of rats that the convulsion was weakened, so it was judged that the seizure had been inhibited. The feasibility of this wireless energy supply system in seizure detection and suppression was verified by recording the LFP and frequency spectrum analysis of rats in normal, epileptic, and light supply conditions.

4 DISCUSSION

Table 2 lists a few seizure detection and inhibition systems published previously. Through the comparison, it can be seen that this study innovatively introduces the optrode into the closed-loop system of seizure detection and suppression. The optrode consists of MEA and LED probes. Compared with the preparation of monolithic integrated optrodes, this preparation method has the following advantages: on the one hand, the MEA and LED probes are prepared on different substrates. The separation of MEA and LED probes in space distance and heavily doped silicon substrate can significantly reduce crosstalk. According to published studies (Fang et al., 2015; Kim et al., 2020; Wang et al., 2021), there are two sources of noise: first, when the wireless energy supply system works, it will introduce electromagnetic interference by supplying power to the LED probe through electromagnetic induction; second, when the LED probe is turned on and illuminated on the silicon substrate, it will produce the photovoltaic effect. The MEA used in the experiment was prepared on a heavily doped silicon substrate, which suppressed noise to a large extent (Wei et al., 2020).

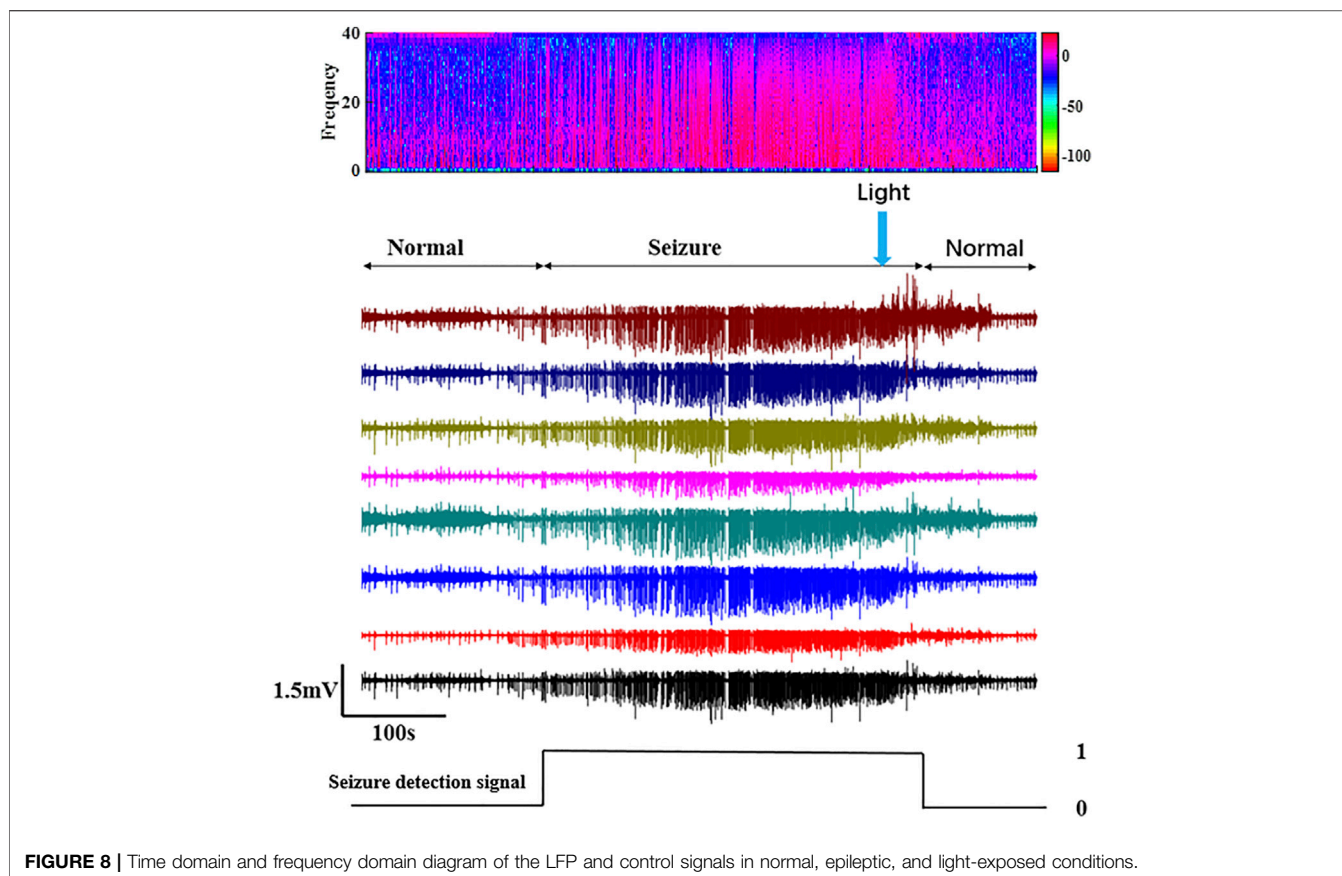


TABLE 2 | Comparison of epilepsy detection systems.

System	Recording	Channels	Stimulation	Ref.
Closed-loop	LFP (Optrode)	8	Light + RuBi-GABA (Optrode)	This work
Closed-loop	LFP (wire electrode)	4	Electric (wire electrode)	Zheng et al. (2019)
Closed-loop	LFP (flexible electrode)	3	Electric (flexible electrode)	Berényi et al. (2012)
Open-loop	EEG (screw electrodes)	2	Light + RuBi-GABA (fiber)	Wang et al. (2017)

On the other hand, the waterproof performance is improved. After the LED probe is prepared, a layer of FDA-certified biocompatible, insulated, waterproof film parylene is encapsulated. The LED encapsulated by parylene can work normally in the sodium chloride solution for more than 60 days.

The seizure detection algorithm of this system distinguishes the normal LFP from epileptic LFP through a threshold judgment. It has the characteristics of fast processing speed and a small amount of calculation, but it has not been entirely accurate. It is difficult to determine the starting point of seizures because of the significant individual differences between rats and the asynchrony of the LFP and behavioral abnormalities. In addition, if abnormalities in the LFP can be detected before a seizure, it can be treated when epileptic behavior does not occur in rats to avoid the occurrence of epileptic behavior. For this exploration, we will refer to other algorithms to improve the real-time and accuracy of seizure recognition. For example, Bolus et al. (Bolus et al., 2021)

established a general framework for continuously modulated closed-loop optogenetic control of neuronal circuits, which applied the state-space linear dynamical system model structure and with linear quadratic optimal control. Fang et al. (Fang and Yang, 2021) also developed a new discrete-time robust and adaptive closed-loop control algorithm. They all significantly improved the performance of the closed-loop control system and provided a method for further study of brain function.

5 CONCLUSION

In this study, a wireless closed-loop optical regulation system for seizure detection and suppression is designed and built. The closed-loop system innovatively combines the electrical signal recording and photosensitive-caged compound therapy and adopts the wireless signal recording, energy supply, and

wireless signal transmission. Through animal experiments, the functions of the whole closed-loop system in LFP real-time monitoring, seizure detection, wireless energy supply, light to release RuBi-GABA, and inhibiting seizures are verified, which provides a new treatment method for epilepsy treatment.

DATA AVAILABILITY STATEMENT

The original contributions presented in the study are included in the article/**Supplementary Material**, further inquiries can be directed to the corresponding authors.

ETHICS STATEMENT

The animal study was reviewed and approved by the Beijing Association on Laboratory Animal Care, license number SYXK (JING)2020–0045.

AUTHOR CONTRIBUTIONS

YL and SX were mainly responsible for the experimental test and manuscript writing. XC, YS, and MW helped in revising the manuscript.

REFERENCES

- Berényi, A., Belluscio, M., Mao, D., and Buzsáki, G. (2012). Closed-Loop Control of Epilepsy by Transcranial Electrical Stimulation. *Science* 337 (6095), 735–737. doi:10.1126/science.1223154
- Bolus, M. F., Willats, A. A., Rozell, C. J., and Stanley, G. B. (2021). State-space Optimal Feedback Control of Optogenetically Driven Neural Activity. *J. Neural Eng.* 18 (3), 036006. doi:10.1088/1741-2552/abb89c
- Bordey, A. (2021). Treating Seizures with Low-Frequency Electrical Stimulation. *Epilepsy Curr.* 21 (3), 197–198. doi:10.1177/15357597211003559
- Chen, S., Pei, W., Zhao, H., Gui, Q., Tang, R., Chen, Y., et al. (2014). 32-site Microelectrode Modified with Pt Black for Neural Recording Fabricated with Thin-Film Silicon Membrane. *Sci. China Inf. Sci.* 57 (5), 1–7. doi:10.1007/s11432-013-4846-1
- Dai, Y., Song, Y., Xie, J., Xiao, G., Li, X., Li, Z., et al. (2020). CB1-Antibody Modified Liposomes for Targeted Modulation of Epileptiform Activities Synchronously Detected by Microelectrode Arrays. *ACS Appl. Mater. Inter.* 12 (37), 41148–41156. doi:10.1021/acsami.0c13372
- Fang, H., and Yang, Y. (2021). “A Robust and Adaptive Control Algorithm for Closed-Loop Brain Stimulation[C]//2021,” in 43rd Annual International Conference of the IEEE Engineering in Medicine & Biology Society (EMBC), Mexico (IEEE), 6049–6052.
- Fang, R., Sun, X., Miao, M., and Jin, Y. (2015). Noise Coupling between Through-Silicon Vias and Active Devices for 20/14-nm Technology Nodes. *AIP Adv.* 5 (4), 041328. doi:10.1063/1.4915322
- Gao, Y., Zheng, J., Jiang, T., Pi, G., Sun, F., Xiong, R., et al. (2021). Targeted Reducing of Tauopathy Alleviates Epileptic Seizures and Spatial Memory Impairment in an Optogenetically Inducible Mouse Model of Epilepsy. *Front. Cell Dev. Biol.* 8, 633725. doi:10.3389/fcell.2020.633725
- Hoffman, C. E., Parker, W. E., Rapoport, B. I., Zhao, M., Ma, H., and Schwartz, T. H. (2020). Innovations in the Neurosurgical Management of Epilepsy. *World Neurosurg.* 139, 775–788. doi:10.1016/j.wneu.2020.03.031
- Hristova, K., Martinez-Gonzalez, C., Watson, T. C., Codadu, N. K., Hashemi, K., Kind, P. C., et al. (2021). Medial Septal GABAergic Neurons Reduce Seizure

FUNDING

This work was sponsored by the National Key Research and Development Program (2017YFA0205903, 2017YFA0701100, and 2017YFA0205902); the National Natural Science Foundation of China (Nos. 61634006, 61671424, 62071447, 62121003, 61960206012, 62121003, 61971400, 61771452, 61775216, 61975206, and 61973292); the strategic priority research program of the CAS pilot project (Nos. XDB32030100 and XDB32040200); the Scientific Instrument Developing Project of the Chinese Academy of Sciences (No. GJJSTD20210004); the Youth Innovation Promotion Association, CAS; and the opening foundation of the State Key Laboratory of Space Medicine Fundamentals and Application, Chinese Astronaut Research and Training Center (No. SMFA19K05).

SUPPLEMENTARY MATERIAL

The Supplementary Material for this article can be found online at: <https://www.frontiersin.org/articles/10.3389/fnano.2022.829751/full#supplementary-material>

Supplementary Figure S1 | The LFP of the control group just for optical stimulation with saline injected.

- Duration upon Optogenetic Closed-Loop Stimulation. *Brain* 144 (5), 1576–1589. doi:10.1093/brain/awab042
- Hu, B., Wang, D., and Shi, Q. (2020). The Effect of External Voltage Stimulation on Absence Seizures[J]. *Technology and Health Care. Amsterdam* 28, S245–S251. Ios Press. doi:10.3233/thc-209025
- Janz, P., Savanthrapadian, S., Häussler, U., Kilias, A., Nestel, S., Kretz, O., et al. (2017). Synaptic Remodeling of Entorhinal Input Contributes to an Aberrant Hippocampal Network in Temporal Lobe Epilepsy. *Cereb. Cortex* 27 (3), 2348–2364. doi:10.1093/cercor/bhw093
- Kawai, K. (2008). Vagus Nerve Stimulation for Intractable Epilepsy: Implantation of Vagus Nerve Stimulator[J]. *Neurological Surgery. Igaku-Shoin Ltd* 36 (11), 979–989. Tokyo.
- Kim, K., Vöröslakos, M., Seymour, J. P., Wise, K. D., Buzsáki, G., and Yoon, E. (2020). Artifact-free and High-Temporal-Resolution *In Vivo* Opto-Electrophysiology with microLED Optoelectrodes. *Nat. Commun.* 11 (1), 2063. doi:10.1038/s41467-020-15769-w
- Klinger, N., and Mittal, S. (2018). Deep Brain Stimulation for Seizure Control in Drug-Resistant Epilepsy. *Amer Assoc. Neurol. Surgeons* 45 (2), E4. doi:10.3171/2018.4.focus1872
- Kozai, T. D. Y., Catt, K., Du, Z., Na, K., Srivannavit, O., Haque, R.-u. M., et al. (2016). Chronic *In Vivo* Evaluation of PEDOT/CNT for Stable Neural Recordings. *IEEE Trans. Biomed. Eng.* 63 (1), 111–119. doi:10.1109/tbme.2015.2445713
- Krishna, V., and Lozano, A. M. (2014). Brain Stimulation for Intractable Epilepsy: Anterior Thalamus and Responsive Stimulation. *Ann. Indian Acad. Neurol.* 17, S95–S98. Mumbai: Wolters Kluwer Medknow Publications. doi:10.4103/0972-2327.128671
- Li, Y., Zhan, L., Wang, Y., Chen, R., Yang, X., Wu, X., et al. (2021). Improve the Spatial Resolution of Fiber Photometry by μ LED Linear Array for Fluorescence Detection. *Sensors Actuators A: Phys.* 331, 112948. doi:10.1016/j.sna.2021.112948
- Long, M. A., and Fee, M. S. (2008). Using Temperature to Analyse Temporal Dynamics in the Songbird Motor Pathway. *Nature* 456 (7219), 189–194. doi:10.1038/nature07448
- Lopes-dos-Santos, V., Campi, J., Filevich, O., Ribeiro, S., and Etchenique, R. (2011). *In Vivo* photorelease of GABA in the Mouse Cortex. *Braz. J. Med. Biol. Res.* 44 (7), 688–693. doi:10.1590/s0100-879x2011007500082

- Mormann, F., Elger, C. E., and Lehnertz, K. (2006). Seizure Anticipation: from Algorithms to Clinical Practice. *Curr. Opin. Neurol.* 19 (2), 187–193. Philadelphia: Lippincott Williams & Wilkins. doi:10.1097/01.wco.0000218237.52593.bc
- Rossetti, A. O., Reichhart, M. D., Schaller, M.-D., Despland, P.-A., and Bogousslavsky, J. (2004). Propofol Treatment of Refractory Status Epilepticus: A Study of 31 Episodes. *Epilepsia* 45 (7), 757–763. doi:10.1111/j.0013-9580.2004.01904.x
- Rothman, S. M., Perry, G., Yang, X. F., Hyrc, K., and Schmidt, B. F. (2007). Optical Suppression of Seizure-like Activity with an LED. *Epilepsy Res.* 74 (2–3), 201–209. doi:10.1016/j.eplepsyres.2007.03.009
- Santhanam, G., Ryu, S. I., Yu, B. M., Afshar, A., and Shenoy, K. V. (2006). A High-Performance Brain-Computer Interface. *Nature* 442 (7099), 195–198. doi:10.1038/nature04968
- Schander, A., Stemann, H., Tolstosheeva, E., Roese, R., Biefeld, V., Kempen, L., et al. (2016). Design and Fabrication of Novel Multi-Channel Floating Neural Probes for Intracortical Chronic Recording. *Sensors Actuators A: Phys.* 247, 125–135. doi:10.1016/j.sna.2016.05.034
- Shen, K.-f., and Schwartzkroin, P. A. (1988). Effects of Temperature Alterations on Population and Cellular Activities in Hippocampal Slices from Mature and Immature Rabbit. *Brain Res.* 475 (2), 305–316. doi:10.1016/0006-8993(88)90619-1
- Sterbova, K., Vickova, M., Klement, P., Neupauerová, J., Staněk, D., Zúnová, H., et al. (2018). Neonatal Onset of Epilepsy of Infancy with Migrating Focal Seizures Associated with a Novel GABRB3 Variant in Monozygotic Twins[J]. *Neuropediatrics* 49 (3), 204–208. Stuttgart: Georg Thieme Verlag Kg. doi:10.1055/s-0038-1626708
- Sun, F. T., and Morrell, M. J. (2014). The RNS System: Responsive Cortical Stimulation for the Treatment of Refractory Partial Epilepsy. *Expert Rev. Med. Devices* 11 (6), 563–572. doi:10.1586/17434440.2014.947274
- Takeuchi, Y., Harangozó, M., Pedraza, L., Földi, T., Kozák, G., Li, Q., et al. (2021). Closed-loop Stimulation of the Medial Septum Terminates Epileptic Seizures. *Oxford* 144, 885–908. Oxford Univ Press. doi:10.1093/brain/awaa450
- Trigo, F. F., Papageorgiou, G., Corrie, J. E. T., and Ogden, D. (2009). Laser Photolysis of DPNI-GABA, a Tool for Investigating the Properties and Distribution of GABA Receptors and for Silencing Neurons *In Situ*. *J. Neurosci. Methods* 181 (2), 159–169. doi:10.1016/j.jneumeth.2009.04.022
- Tsai, J.-D., Fan, P.-C., Lee, W.-T., Hung, P. L., Hung, K. L., Wang, H. S., et al. (2020). Vagus Nerve Stimulation in Pediatric Patients with Failed Epilepsy Surgery[J]. *Acta Neurol. Belgica* 121 (5), 1305–1309. doi:10.1007/s13760-020-01303-8
- Wang, D., Yu, Z., Yan, J., Xue, F., Ren, G., Jiang, C., et al. (2017). Photolysis of Caged-GABA Rapidly Terminates Seizures *In Vivo*: Concentration and Light Intensity Dependence. *Front. Neurol.* 8, 215. doi:10.3389/fneur.2017.00215
- Wang, M., Guo, B., Ji, B., Fan, Y., Wang, L., Ye, L., et al. (2021). Controlled Electrodeposition of Graphene Oxide Doped Conductive Polymer on Microelectrodes for Low-Noise Optogenetics. *IEEE Electron. Device Lett.* 42 (3), 418–421. doi:10.1109/led.2021.3051617
- Wei, C., Wang, F., Pei, W., Liu, Z., Mao, X., Zhao, H., et al. (2020). Light-Induced Noise Reduction of Lightly Doped Silicon-Based Neural Electrode. *Acta Physico Chim. Sinica* 36 (0), 2005033. doi:10.3866/pku.whxb202005033
- White, A. M., Williams, P. A., Ferraro, D. J., Clark, S., Kadam, S. D., Dudek, F. E., et al. (2006). Efficient Unsupervised Algorithms for the Detection of Seizures in Continuous EEG Recordings from Rats after Brain Injury. *J. Neurosci. Methods* 152 (1–2), 255–266. doi:10.1016/j.jneumeth.2005.09.014
- Xu, K., Zheng, Y., Zhang, F., Jiang, Z., Qi, Y., Chen, H., et al. (2019). An Energy Efficient AdaBoost Cascade Method for Long-Term Seizure Detection in Portable Neurostimulators. *IEEE Trans. Neural Syst. Rehabil. Eng.* 27 (11), 2274–2283. doi:10.1109/tnsre.2019.2947426
- Yang, X.-F., Schmidt, B. F., Rode, D. L., and Rothman, S. M. (2010). Optical Suppression of Experimental Seizures in Rat Brain Slices. *Epilepsia* 51 (1), 127–135. doi:10.1111/j.1528-1167.2009.02252.x
- Yang, X., Rode, D. L., Peterka, D. S., Yuste, R., and Rothman, S. M. (2012). Optical Control of Focal Epilepsy *In Vivo* with Caged γ -aminobutyric Acid. *Ann. Neurol.* 71 (1), 68–75. doi:10.1002/ana.22596
- Yang, Y., Lee, J. T., Guidera, J. A., Vlasov, K. Y., Pei, J., Brown, E. N., et al. (2019). Developing a Personalized Closed-Loop Controller of Medically-Induced Coma in a Rodent Model. *J. Neural Eng.* 16 (3), 036022. doi:10.1088/1741-2552/ab0ea4
- Zhang, H., Pei, W., and Yang, X. (2016). “A Sapphire Based Monolithic Integrated Optrode[C]//2016 38th,” in Annual International Conference of the IEEE Engineering in Medicine and Biology Society (EMBC), Orlando, FL, USA (IEEE), 6186–6189.
- Zheng, Y., Jiang, Z., Ping, A., Zhang, F., Zhu, J., Wang, Y., et al. (2019). Acute Seizure Control Efficacy of Multi-Site Closed-Loop Stimulation in a Temporal Lobe Seizure Model. *IEEE Trans. Neural Syst. Rehabil. Eng.* 27 (3), 419–428. doi:10.1109/tnsre.2019.2894746

Conflict of Interest: The authors declare that the research was conducted in the absence of any commercial or financial relationships that could be construed as a potential conflict of interest.

Publisher’s Note: All claims expressed in this article are solely those of the authors and do not necessarily represent those of their affiliated organizations, or those of the publisher, the editors, and the reviewers. Any product that may be evaluated in this article, or claim that may be made by its manufacturer, is not guaranteed or endorsed by the publisher.

Copyright © 2022 Li, Xu, Wang, Duan, Jia, Xie, Yang, Wang, Dai, Yang, Yuan, Wu, Song, Wang, Chen, Wang, Cai and Pei. This is an open-access article distributed under the terms of the Creative Commons Attribution License (CC BY). The use, distribution or reproduction in other forums is permitted, provided the original author(s) and the copyright owner(s) are credited and that the original publication in this journal is cited, in accordance with accepted academic practice. No use, distribution or reproduction is permitted which does not comply with these terms.